Drag force modelling in dilute to dense particle-laden flows with mono-disperse or binary mixture of solid particles

Olivier Simonin, Solène Chevrier, François Audard, Pascal Fede

Drag force modelling in dilute to dense particle-laden flows with mono-disperse or binary mixture of solid particles

Olivier Simonin, Solène Chevrier, François Audard, Pascal Fede
Institut de Mécanique des Fluides de Toulouse (IMFT), Université de Toulouse, CNRS, INPT, UPS, Toulouse FRANCE

Abstract

Fluid-particle momentum transfer modelling is a key issue for the simulation of gas-solid fluidized beds. In the literature, many empirical correlations can be found for the prediction of the drag force but these correlations are generally not satisfactory for all the flow conditions found in fluidized bed: dilute and dense regime, low and high particle Reynolds number values, mono- or poly-disperse solid mixture. Up to now, in dense particulate flows, the validation of such correlations were performed only by comparison with experiments using mean pressure drop, fluidization or settling velocity measurements and analytical solutions in some limit cases (Stokes flow). Nowadays, the development of particle resolved numerical techniques, like Lattice Boltzmann Method (LBM), allows to perform Direct Numerical Simulation (DNS) of the flow across dilute and dense particle arrays. Such simulations allow to compute directly the forces acting on the particles which may be used to validate or develop drag force correlations. In the present paper, we show that the simple drag correlation proposed by Gobin et al. (2003) [6], and already used extensively for circulating and dense fluidized bed simulation, is in very good agreement with the particle-resolved immersed boundary-method results of Tenneti et al. (2011)[15] and with the boddy-fitted DNS results of Massol [10]. An extension of the correlation is also proposed for poly-disperse mixture based on the LBM results of Beetstra et al. (2007)[1].

Keywords: Drag law, Dense fluidized bed, Gas-particles flows , Polydisperse

1. Introduction

Multiphase flow reactors are commonly used in many industrial processes such as chemical polymerization reactors or fluid catalytic cracking unit. Due to computational limitations, the effective modelling approach used for industrial scale reactor simulations is usually considering the fluid and particle phases as continuous and interacting media governed by locally averaged equations (Euler-Euler approach). For applications with a limited number of particles, or using the Monte-Carlo method, it is also possible to track the positions and the velocities of discrete particles by coupling with a continuous averaging approach for the fluid (Eulerian-Lagrangian approach). In those approaches, constitutive relations are used to take into account unknown terms appearing from the averaging, fluid-particle drag, lift, history, added-mass force. For gas-solid flows, the fluid-particle drag force has a dominant influence on the hydrodynamic behaviour of the flow and the simulation accuracy is strongly dependant on the fluid-particle drag constitutive relation. Therefore, closures for the fluid-particle drag force have been investigated since the 20^{th} century. Empirical correlation [3, 18] are the most widely used to close the fluid-solid drag force. Theoretically some authors [7, 11] have demonstrated models in specific configuration for periodic fixed sphere, for low volume fraction and low Reynolds number. However their domains of validity are very limited and those models cannot be used to model the industrial-scale reactors. There is also a further difficulty when the polydispersion effect has to be taken into account. Recently, the development of numerical techniques, such as body-fitted CFD, fictious domain approach, Lattice Boltzmann Method (LBM) and Immersed Boundary Method (IBM), allows to perform DNS of the flow across dilute and dense particle arrays. Such simulations lead to compute directly the forces acting on the particles which may be used to validate or develop drag force correlations.

This article focuses on a comparison between fluid-particle drag prediction for monodisperse flows and for polydisperse flows found in the literature. In monodisperse cases, an analysis is done on models found in the literature [3, 18, 6, 1, 19] correlation and the DNS data of Ref. [8, 9, 16, 1, 12] and the body-fitted CFD data of Ref. [10]. In polydisperse cases, an analysis is done on the extension developed by Beetstra et al. and Yin et al. and an extension is proposed based on the LBM results of Beetstra et al.

2. Modelling of momentum transfer into gas-particle flow

Let us define $F_{fp,i}$ the local average force exerted by the fluid on the particles of section p in polydisperse powder. In the frame of the Euler-Euler approach for gas-particle flows [14], such a force is usually written has the sum of two contributions: the drag force, $F^D_{fp,i}$ and the buoyancy force,

$$F_{fp,i} = F^D_{fp,i} - V_p \frac{\partial P_f}{\partial x_i} \tag{1}$$

where $\partial P_f / \partial x_i$ is the mean fluid pressure gradient, and $V_p = \pi d_p^3/6$ is the volume of the particle of diameter d_p. Then, the fluid momentum transport equation writes:

$$\begin{aligned} \alpha_f \rho_f \frac{\partial U_{f,i}}{\partial t} + \alpha_f \rho_f U_{f,j} \frac{\partial U_{f,i}}{\partial x_j} = & - \alpha_f \frac{\partial P_f}{\partial x_i} \\ & + \alpha_f \frac{\partial \Sigma_{f,ij}}{\partial x_j} \\ & + \alpha_f \rho_f g_i \\ & - \sum_q n_q F^D_{fq,i} \end{aligned} \tag{2}$$

where $\sum_q$ means that the summation is performed over all particulate diameter distribution. For steady flow through arrays of fixed particles, and without gravity, the equation becomes

$$-\alpha_f \frac{\partial P_f}{\partial x_i} - \sum_q n_q F^D_{fq,i} = 0 \tag{3}$$

Let us introducing the following quantities

$$x_p = \frac{\alpha_p}{\alpha_s} \qquad \text{and} \qquad y_p = \frac{d_p}{d_s}, \tag{4}$$

where α_s is the whole particle volume fraction ($\alpha_s = \sum_q \alpha_q$) and d_s is the Sauter's diameter given by

$$d_s = \left[\sum_p \frac{x_p}{d_p}\right]^{-1} . \tag{5}$$

Then the total force measured in fully-resolved simulation can be related to the drag force by equating Eqn (3) & (4) as

$$F_{fp,i} = F^D_{fp,i} + \frac{\alpha_s}{\alpha_f} y_p^3 \sum_q \frac{x_q}{y_q^3} F^D_{fq,i} . \tag{6}$$

For the monodisperse case, $x_p = 1$ and $y_p = 1$, the expression becomes

$$F_{fp,i} = \frac{1}{\alpha_f} F^D_{fp,i} . \tag{7}$$

In Ref. [1, 16, 12] the mean force exerted by the fluid on the particle is measured from LBM simulations allowing to derive several fluid force correlatons. Finally, in the following, we will evaluate drag force correlations derived using various DNS approaches for dense suspension of monodisperse and polydisperse solid mixture.

3. Drag force in a fixed array of mono-sized spherical solid particles

The mean drag force in a fixed array of mono-sized solid spheres may be written,

$$F^D_{fp,i} = -\rho_f \frac{\pi d_p^2}{8} C_D |\mathbf{V}_r| V_{r,i} \tag{8}$$

with d_p the particle diameter, ρ_f the fluid density, $\mathbf{V}_r = \mathbf{U}_p - \mathbf{U}_f$ the mean fluid-particle relative velocity and $C_D \equiv C_D(Re_p)$ the drag coefficient. The drag coefficient depends on the particle Reynolds number Re_p that is defined by

$$Re_p = \frac{|\mathbf{V}_r| d_p}{\nu_f} . \tag{9}$$

For a single particle ($\alpha_f = 1$) the drag force in the Stokes limit ($Re_p \ll 1$) is written,

$$F^D_{fp,i} = -3\pi \rho_f \nu_f d_p V_{r,i} . \tag{10}$$

Then the drag coefficient C_D in the Stokes regime is given by,

$$C_D = \frac{24}{Re_p} \tag{11}$$

Practical correlations of the drag coefficient may be found in the literature such as the one proposed by Schiller & Naumann [13] which is extensively used in gas-solid flow simulation.

By analogy with the form of a single particle drag force, Eqn (8), the drag force in dense particle laden flows is written as

$$F^D_{fp,i} = -\rho_f \frac{\pi d_p^2}{8} C^*_D |\mathbf{V}_r| V_{r,i} \tag{12}$$

where the drag coefficient $C^*_D \equiv C^*_D(Re^*_p, \alpha_f)$ is a given function of the particle Reynolds number Re^*_p and of α_f the fluid volume fraction.

$$Re^*_p = \frac{\alpha_f |\mathbf{V}_r| d_p}{\nu_f} . \tag{13}$$

The semi-empirical popular correlations given by Ergun [3] and Wen & Yu [18] are evaluated in this section for mono-sized particles. Ding & Gidaspow [2] proposed a correlation with a transition from the Wen & Yu to the Ergun correlations for $\alpha_s > 0.2$. However this correlation leads to discontinuous transition and overestimation of the drag force for $\alpha_s > 0.2$ and for the particle Reynolds number > 100 encountered in gas phase olefin polymerization reactor. This leads to Gobin & al. [6] propose a continuous transition given in Tab. 1 according to the DNS results of Massol [10]. Recently, new forms for the monodisperse drag force correlation were derived from DNS results such as the ones proposed by Beetstra et al. [1] and Tenneti et al. [15], given in Tab. [1]. Table [1] shows the different correlation proposed by the different author in the literature. For all results presented the drag force are normalized by the Stokes drag force,

$$F^D(\alpha_f, Re^*_p) = \frac{|\mathbf{F}^D_{fp}|}{3\pi\mu_f d_p \alpha_f |\mathbf{V_r}|} \tag{14}$$

Figure 1, shows the dimensionless drag force for low particle Reynolds number (Re^*_p =1) as a function of the solid volume fraction, the line represent the correlations given in Table [1] and the black symbols are the LBM numerical results from [8]. For volume fraction larger than 0.1, LBM results are found in good agreement with theoretical developments made by [7, 11], Gobin et al. correlation (ie. Wen & Yu and Ergun) leads to an underestimation of the drag force with respect to the LBM results of Hill et al.

This theoretical developments are valid for fixed bed, in cubic arrays configuration (simple, body-centered and face-centered), Hill et al. [8, 9] shown this theory are valid for random array. In contrast when the particles are not frozen, the behaviour of flow could be changed, and the drag force acting on the particle are not strictly equivalent to a fixed bed.

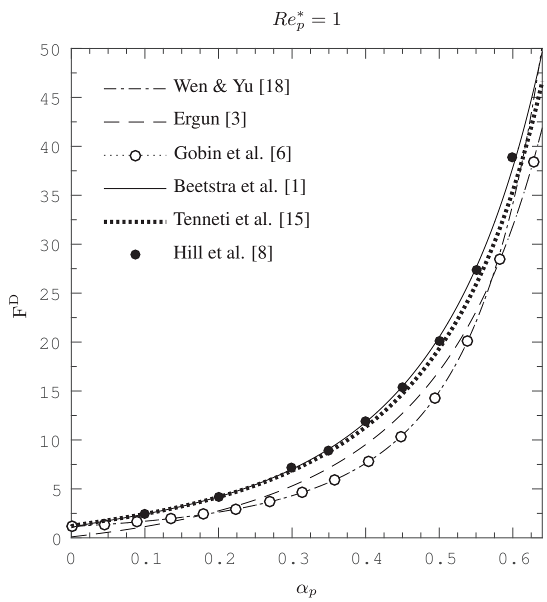

Figure 1: Comparison between the LBM and the different equations of dimensionless drag force apply in a fixed array of mono-sized spherical solid particles (see Tab. [1]) (without the pressure gradient) as a function of the particle volume fraction α_p for $Re^*_p = 1$.

Figure 2, shows the dependence of the dimensionless drag force on the solid volume fraction for several particle Reynolds numbers Re_p, comparing the predictions of the correlation functions given Table [1] and the DNS results with a body fitted mesh by Massol [10]. Results using Tenneti et al. correlation [15] and

Table 1: Relations for the normalized drag force of a monodisperse system, as function of gas volume fraction and Reynolds number $Re_p^* = \alpha_f |\mathbf{V}_r| d_p / \nu_f$

Author	Drag force
Ergun 1952 [3]	$F^D_{Erg} = \frac{150}{18}\frac{1-\alpha_f}{\alpha_f^2} + \frac{7}{4}\frac{1}{18}\frac{Re_p^*}{\alpha_f^2}$
Wen and Yu 1965 [18]	$F^D_{WY} = (1 + 0.15 Re_p^{*0.687})\alpha_f^{-3.65}$
Gobin et al. 2003 [6]	$F^D_{Gob} = \begin{cases} F^D_{WY} & \text{if} \quad \alpha_p \leq 0.3 \\ min(F^D_{WY}, F^D_{Erg}) & \text{otherwise} \end{cases}$
Beetstra, Van der Hoef & Kuipers 2007 [1]	$F^D_{BVK} = 10\frac{1-\alpha_f}{\alpha_f^2} + \alpha_f^2(1+1.5\sqrt{1-\alpha_f}) + \frac{0.413}{\alpha_f^2}\frac{Re_p^*}{24}\left[\frac{\alpha_f^{-1} + 3\alpha_f(1-\alpha_f) + 8.4 Re_p^{*-0.343}}{1 + 10^{3(1-\alpha_f)} Re_p^{*-0.5-2(1-\alpha_f)}}\right]$
Tenneti et al. 2011 [15]	$F^D_{TGS} = F^D_{WY}(Re_p^*)\alpha_f^{1.65} + \alpha_f F_1(\alpha_f) + \alpha_f F_2(\alpha_f, Re_p^*)$
	$F_1(\alpha_f) = \frac{5.81(1-\alpha_f)}{\alpha_f^3} + 0.48\frac{(1-\alpha_f)^{1/3}}{\alpha_f^4}$
	$F_2(\alpha_f, Re_p^*) = (1-\alpha_f)^3 Re_p^* \left[0.95 + \frac{0.61(1-\alpha_f)^3}{\alpha_f^2}\right]$

DNS results from Massol [10] are very closed. We can notice that Tenneti et al correlations are fitted from DNS results obtained using immersed boundary methods (IBM).

Gobin et al. [6] drag force correlation predictions, are really closed to the Massol DNS results for the whole range of particle Reynolds number and particle volume fraction shown. In particular, the proposed transition model from Wen & Yu to Ergun correlations allows to predict accurately the drag force in dense particle-laden flows for large particle Reynolds number values : $Re_p^* \geq 100$. Hence, to develop a correlation for polydisperse systems, a simple polydispersed correlation based Gobin et al. [6] mono-sized drag force will be presented and evaluated.

4. Drag force in a fixed array of polydisperse spherical solid particles

Some authors, like Van der Hoef [16] and Yin and Sundaresan [19], developed polydisperse models using the monodisperse force applied to a mean diameter corrected by a function of the particle mixture properties. Van der Hoef et al. [16] propose the following form for the normalized by Stokes force drag force for particle type p,

$$F^D_{VBK,poly} = f_{poly}(\alpha_f, y_p) {F_{BVK}}^D(\alpha_f, Re_s^*) \quad (15)$$

with $f_{poly}(\alpha_f, y_p)$ written as,

$$f_{poly}(\alpha_f, y_p) = \alpha_f y_p + (1-\alpha_f) y_p^2$$

Re_s^* is the Reynolds number using the Sauter's diameter, written:

$$Re_s^* = \frac{\alpha_f |\mathbf{V}_r| d_s}{\nu_f}. \quad (16)$$

Yin and Sundaresan 2009[19] propose the following form,

$$F^D_{YS,poly} = C_1 + f_{poly}(\alpha_f, y_p) F^D_{VBK}(\alpha_f, Re_s^*) \quad (17)$$

$$f_{poly}(\alpha_f, y_p) = a y_p + (1-a) y_p^2$$

$$a = 1 - 2.660(1-\alpha_f) + 9.096(1-\alpha_f)^2 - 11.338(1-\alpha_f)^3$$

$$C_1 = \frac{1}{\alpha_f} + \frac{1}{\alpha_f}[a y_p + (1-a) y_p^2]$$

The monosdiperse force F^D_{VBK} corresponds to the correlaiton developed by Van der Hoef et al. [16],

$$F^D_{VBK} = 10\frac{1-\alpha_f}{\alpha_f^2} + \alpha_f^2(1 + 1.5\sqrt{1-\alpha_f}) \quad (18)$$

The Gobin et al. drag force correlation was already used for Euler-Euler numerical simulation of laboratory and industrial scale gas-solid polydisperse fluidized bed [4, 5]. The corresponding dimensionless drag force takes the following form,

$$F^D_{Gob,poly} = y_p F^D_{Gob}(\alpha_f, y_p Re_s^*) \quad (19)$$

A second form more complex, accounting the separate dependence on the diameter ratio y_p and the gas volume fraction α_f is proposed. The function is determined by a fitting with the LBM data using the least-squares methods,

$$F^D_{2,Gob,poly} = f_{poly}(\alpha_f, y_p) F^D_{Gob}(\alpha_f, y_p Re_s^*) \quad (20)$$

The function is determined by a fitting with the LBM data using the least-squares methods,

$$f_{poly} = y_p + 0.1(y_p - 1)((y_p^{1.5} - 1) + \alpha_f(1.25 - 5\alpha_f)).$$

This correlation focus only on the range [0:100] of particle Reynolds number.

Figure 3, shows the normalized polydisperse drag force divided by the normalized monodisperse drag force. These monodisperse force for each case has been calculated with the Reynolds number depending on the Sauter's diameter Re_s^*. The Figure shows the dependence of the normalized polydisperse drag force coefficient on the particle diameter ratio y_p, for given values of the Reynolds number Re_s^* and of the gas volume fraction α_f. The different line corresponds to the correlations by the Eqn (15), (17), (19) & (20). The point represents the LBM numerical data given by these different authors [1, 12]. $F^D_{Gob,poly}$

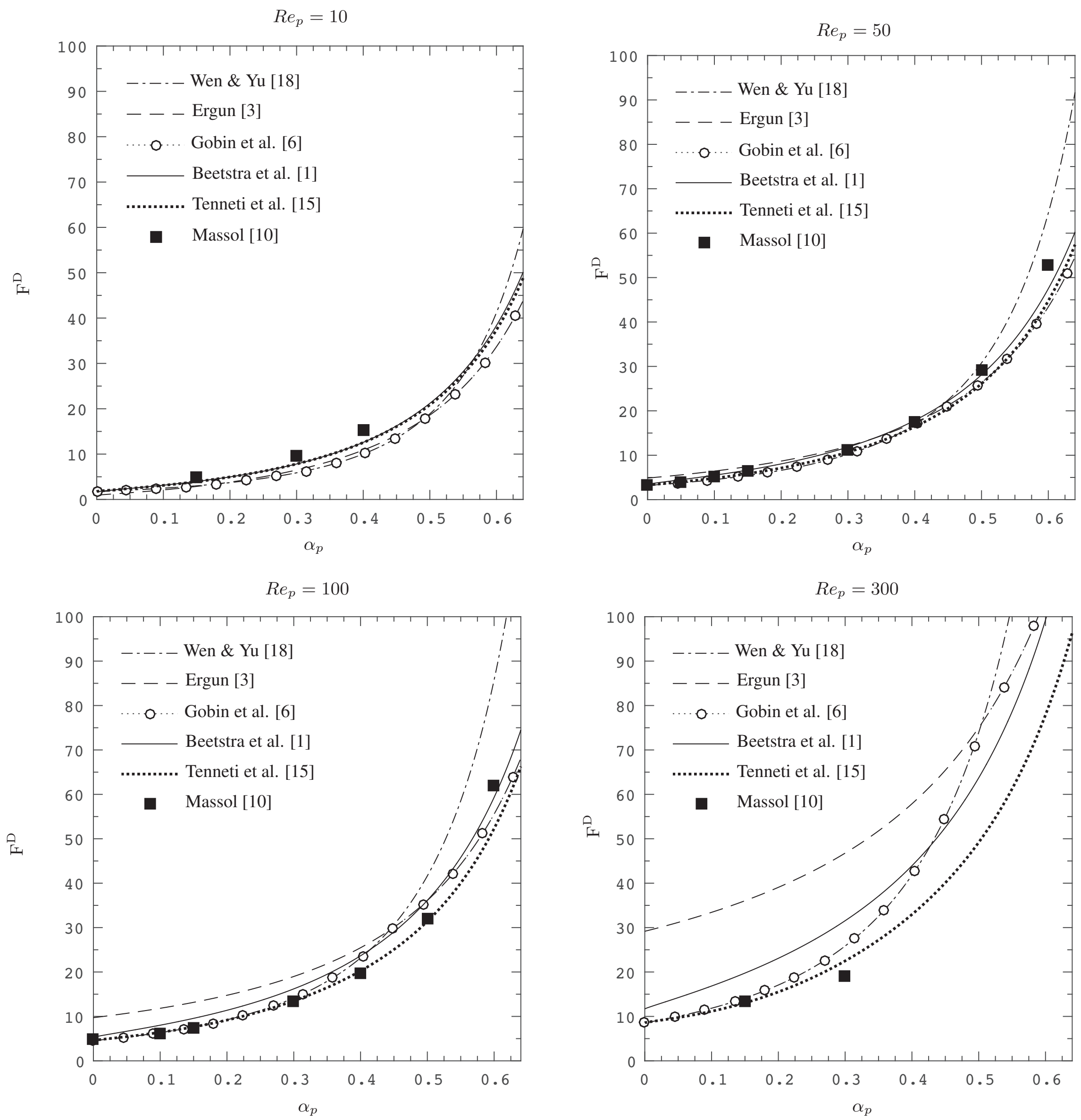

Figure 2: Comparison between the DNS and the different equations of dimensionless drag force (see Tab. [1]) (without the pressure gradient) as a function of of the gas volume fraction α_f for different Reynolds number Re_p apply in a fixed array of mono-sized spherical solid particles.

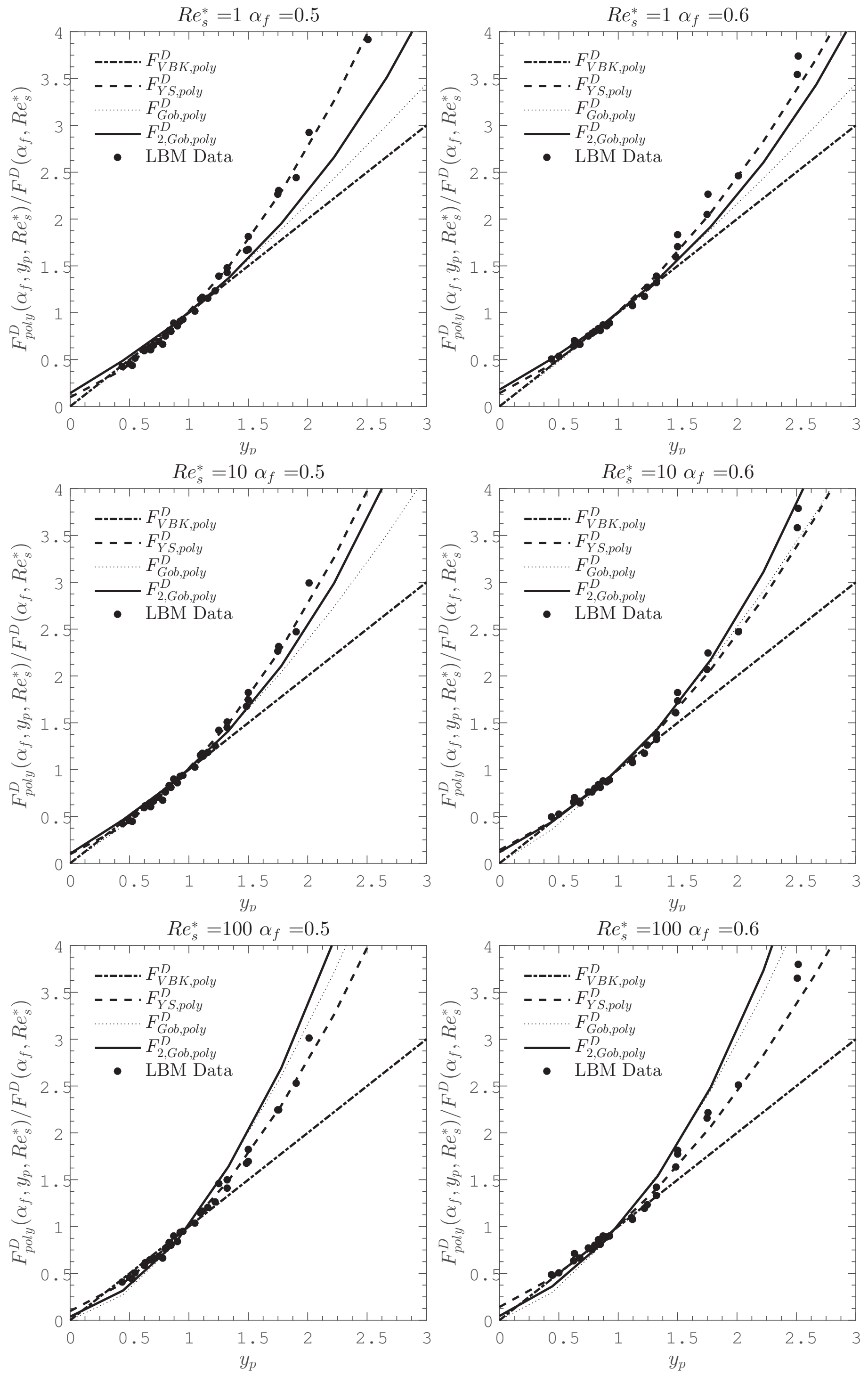

Figure 3: Comparison between LBM data [1] [12] and the correlations and the new correlation written in section 4. The vertical axis corresponds to the dimensionless drag force normalized by the dimensionless monodisperse drag force using the Reynolds number based on mean Sauter diameter Re_s^*; the horizontal axis is the dimensionless particle size ratio y_p.

and $F^D_{2,Gob,poly}$ represent the models given in Eqn (19) and (20). All correlation are equal to the monodisperse drag force when the diameter is equal to the Sauter 's diameter, $y_p = 1$. For low $Re_s^* = 1$, The simple Gobin et al. correlation corresponding to $F^D_{Gob,poly}$, shows a good agreement with the LBM data. In contrast, the results for higher Re_s^* shows an underestimation by this simple model.

5. Conclusion

The drag force correlations developed from DNS results using Lattice Boltzmann Method (LBM) [1] and semi-empirical functions found in the literature (Ergun [3], Wen & Yu et al. [18], Gobin et al. [6], were compared for monodisperse flows. The correlation of Gobin et al.[6] provides satisfactory predictions and maximum discrepancies are measured for low Reynolds number values. For polydisperse flows several correlations may be found in the literature to take into account the dependence on the particle diameter ratio, the particle Reynolds number and the solid volume fraction, likes the ones of Van der Hoef [16] and of Yin and Sundaresan [19]. The different authors proposed for polydisperse drag force to multiply the monodisperse drag force calculated with the Sauter mean diameter by a function depending on particle size ratio y_p and gas volume fraction. The results provided by a polydisperse applicaiton of the Gobin et al. [6] correlation tend to slightly underestimated the drag force compared to the LBM results of Beetstra [1] and to the others correlation developed for polydisperse flows [16, 19] for low Reynolds $Re_s^* \leq 10$. An overestimation of the drag force is observed for large Reynolds number value $Re_s^* = 100$. LBM data represent frozen particle suspension in a steady gas flow, but the gas-solid suspensions are usually unstable. The particle-particle relative motion and particle-turbulence interactions should modify the drag force correlation modelling. So, additional numerical studies using unsteady particle resolved simulation allowing separate particle motion [17] are needed to improve the drag force modelling accuracy in fluidized beds.

References

[1] R. Beetstra, M.A. Van der Hoef, and J.A.M. Kuipers. Drag force of intermediate reynolds number flow past mono- and bidisperse arrays of spheres. *AIChE Journal*, 53:489–501, 2007.

[2] J. Ding and D. Gidaspow. A bubbling fluidization model using kinetic theory of granular flow. *AIChE Journal*, 36(4):523–538, 1990.

[3] S. Ergun. Fluid flow through packed columns. *Chemical Engineering Progress*, 48:89–94, 1952.

[4] P. Fede, O. Simonin, and I. Ghouila. 3d numerical simulation of polydisperse pressurized gas-solid fluidized bed. In *ASME-JSME-KSME 2011 Joint Fluids Engineering Conference*, pages 3199–3210. American Society of Mechanical Engineers, 2011.

[5] F. Fotovat, R. Ansart, M. Hemati, O. Simonin, and J. Chaouki. Sand-assisted fluidization of large cylindrical and spherical biomass particles: Experiments and simulation. *Chemical Engineering Science*, 126:543–559, 2015.

[6] A. Gobin, H. Neau, O. Simonin, J. R. Llinas, V. Reiling, and J. L. Sélo. Fluid dynamic numerical simulation of a gas phase polymerisation reactor. *International Journal for Numerical Methods in Fluids*, 43:1199–1220, 2003.

[7] H. Hasimoto. On the periodic fundamental solutions of the stokes equations and their application to viscous flow past a cubic array of spheres. *Journal of Fluid Mechanics*, 5(02):317–328, 1959.

[8] R.J. Hill, D.L. Koch, and A. J.C. Ladd. The first effects of fluid inertia on flows in ordered and random arrays of spheres. *Journal of Fluid Mechanics*, 448:213–241, 2001.

[9] R.J. Hill, D.L. Koch, and A.J.C. Ladd. Moderate-reynolds-number flows in ordered and random arrays of spheres. *Journal of Fluid Mechanics*, 448:243–278, 2001.

[10] A. Massol. *Simulations numériques d'écoulements à travers des réseaux fixes de sphères monodisperses et bidisperses, pour des nombres de Reynolds modérés*. PhD thesis, INPT - CERFACS, 2004.

[11] A.S. Sangani and A. Acrivos. Slow flow through a periodic array of spheres. *International Journal of Multiphase Flow*, 8(4):343–360, 1982.

[12] S. Sarkar, M.A. Van der Hoef, and J.A.M. Kuipers. Fluid–particle interaction from lattice boltzmann simulations for flow through polydisperse random arrays of spheres. *Chemical Engineering Science*, 64(11):2683–2691, 2009.

[13] L. Schiller and A. Nauman. A drag coefficient correlation. *V.D.I. Zeitung*, 77:318–320, 1935.

[14] O. Simonin. Combustion and turbulence in two-phase flows. In *Lecture Series 1996-02*. Von Karman Institute for Fluid Dynamics, 1996.

[15] S. Tenneti, R. Garg, and S. Subramaniam. Drag law for monodisperse gas–solid systems using particle-resolved direct numerical simulation of flow past fixed assemblies of spheres. *International journal of multiphase flow*, 37(9):1072–1092, 2011.

[16] M.A. Van der Hoef, R. Beetstra, , and J.A.M. Kuipers. Lattice-boltzmann simulations of low-reynolds-number flow past mono- and bidisperse arrays of spheres: results for the permeability and drag force. *Journal of Fluid Mechanics*, 528:233–254, 4 2005.

[17] S. Vincent, J.C.B. De Motta, A. Sarthou, J.L. Estivalezes, O. Simonin, and E. Climent. A lagrangian vof tensorial penalty method for the dns of resolved particle-laden flows. *Journal of Computational Physics*, 256:582–614, 2014.

[18] Y.C. Wen and Y.H. Yu. Mechanics of fluidization. *Chemical Engineering Symposium Series*, 62:100–111, 1965.

[19] X. Yin and S. Sundaresan. Fluid-particle drag in low-reynolds-number polydisperse gas-solid suspensions. *AIChE Journal*, 55:1352–1368, 2009.